

Different Approaches to Low-Wettable Materials for Freezing Environments: Design, Performance and Durability

Giulio Boveri, Alessandro Corozzi *, Federico Veronesi and Mariarosaa Raimondo

Institute of Science and Technology for Ceramics, National Research Council (ISTEC CNR), Via Granarolo, 64, 48,018 Faenza, Italy; giulioboveri01@gmail.com (G.B.); federico.veronesi@istec.cnr.it (F.V.); mariarosaa.raimondo@istec.cnr.it (M.R.)

* Correspondence: alessandro.corozzi@istec.cnr.it; Tel.: +39-0546-699-776

1. Freeze and Frost Cycles on SLIPS surfaces

In the case of frosting on SLIP surfaces, water drops are free to move in every direction and they first nucleate on the free surface of the lubricant [1]. Since the drops are small, in the early stage one can neglect gravity. After some time, the drops grew in size. Due to gravity the drops begin to sink until their bottom comes into contact with the substrate forming a three-phase contact line between water/lubricant/substrate. The creation of this solid contact line is the cause of the surface pinning. If pinned neighboring drops grew large enough that the lubricant menisci start overlapping a net attractive force between each other arises. Such phenomenon is similar to the lateral attraction between two particles which are suspended on a free liquid surface [2]. The consequent coalescence drives lubricant transport to the lateral directions (See Scheme S1).

During the freeze/thaw cycles the same lubricant transport to the lateral direction is extreme so as it is the lubricant drainage from the surface porosity because of the amount of pressure exerted by the water column. As seen from the SEM micrograph in Figure S1., the transport phenomena during the freezing cycle leads to the accumulation of lubricant on the border of the freezing zone. We presume that the drainage of lubricant out the freezing area is the main responsible for the loss of anti-wetting properties.

Citation: Boveri, G.; Corozzi, A.; Veronesi, F.; Raimondo, M. Different Approaches to Low-Wettable Materials for Freezing Environments: Design, Performance and Durability. *Coatings* **2021**, *1*, 77. <https://doi.org/10.3390/coatings11010077>

Received: 23 December 2020

Accepted: 5 January 2021

Published: 11 January 2021

Publisher's Note: MDPI stays neutral with regard to jurisdictional claims in published maps and institutional affiliations.



Copyright: © 2021 by the authors. Submitted for possible open access publication under the terms and conditions of the Creative Commons Attribution (CC BY) license (<http://creativecommons.org/licenses/by/4.0/>).

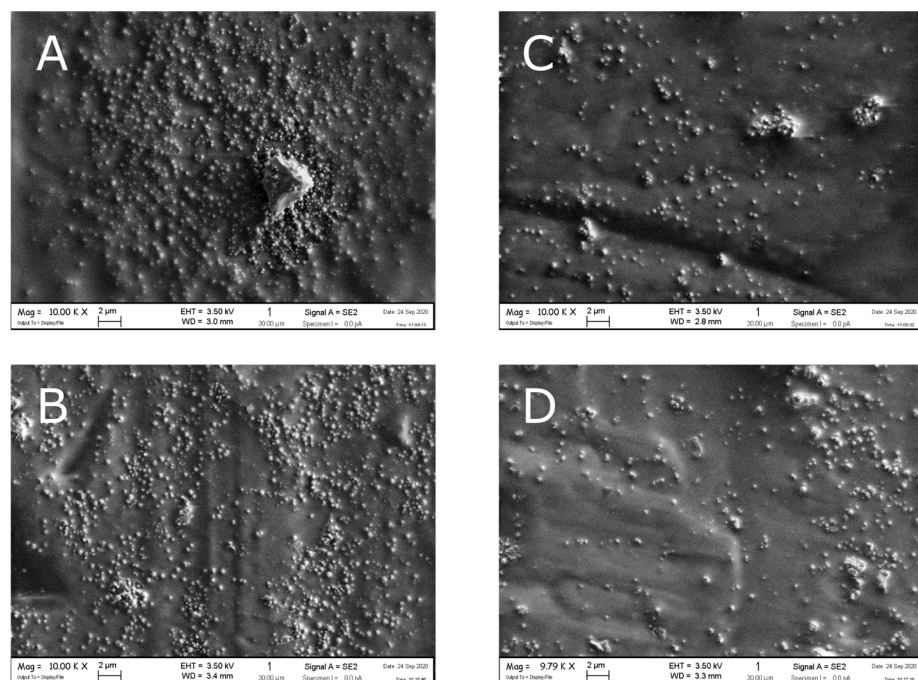
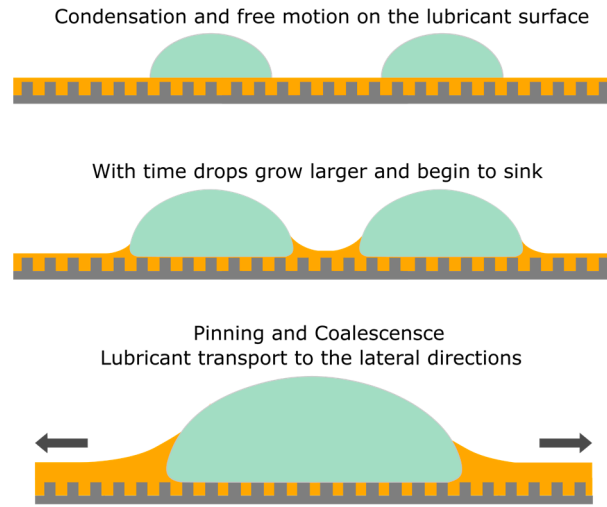


Figure 1. (a) SEM micrograph of the freezing zone of SiO₂/SO10 surface after freeze/thaw test; (b) SEM micrograph of the freezing zone of SiO₂/Kr105 surface after freeze/thaw test; (c) and (d) are

instead reported as example of lubricant accumulation on the border zones for SiO₂/SO10 and SiO₂/Kr105 respectively.



Scheme 1. Pinning and coalescence freezing.

2. Calculation of the Hamaker Constant:

The original Lifshitz theory Dzyaloshinskii-Lifshitz-Pitaevskii (DLP) theory is a classical theory derived as a generalisation of quantum field theory. Within this theory the atomic structure is ignored and the forces between large bodies - now treated as continuous media - are derived in terms of bulk properties as dielectric constants and refractive indices. In the planar "asymmetric configuration", i.e. two phases a and c interacting across medium b (See Scheme S2), the complete expression for the nonretarded Hamaker constant based on the DLP theory is [3,4]:

$$\mathcal{A} \approx \frac{3}{4} k_B T \frac{(\epsilon_a - \epsilon_c)(\epsilon_b - \epsilon_c)}{(\epsilon_a + \epsilon_c)(\epsilon_b + \epsilon_c)} + \frac{3h}{4\pi} \int_{\xi_1}^{\infty} \left[\frac{\epsilon_a(i\xi) - \epsilon_c(i\xi)}{\epsilon_a(i\xi) + \epsilon_c(i\xi)} \right] \left[\frac{\epsilon_b(i\xi) - \epsilon_c(i\xi)}{\epsilon_b(i\xi) + \epsilon_c(i\xi)} \right] d\xi \quad (1)$$

Where:

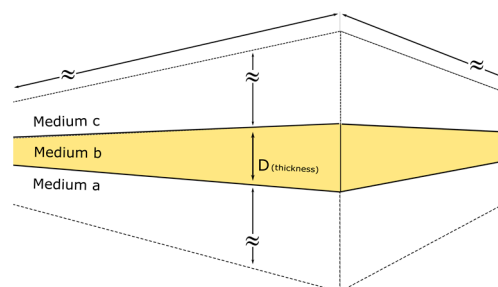
ϵ_i are the static dielectric constants with index $i = a, b, c$ (the three media);

$\epsilon_i(i\xi)$ are the values of ϵ_i at imaginary frequencies with index $i = a, b, c$;

k_B is the Boltzmann Constant;

h is the Plank Constant.

The first term of Equation (1) gives the zero-frequency energy of the van der Waals interaction and includes the Keesom and Debye contributions. The second term gives the dispersion energy and it includes the London energy contribution. The equation is not exact, because it is the first term in an infinite series, anyhow the other terms are small and they generally contribute no more than 5%.



Scheme S2. Semi-infinite layers of two mediums a and c acting across a medium b of thickness D.

If we assume that i) the dispersion energy is largely determined by the electronic absorption only, and ii) the absorption frequencies of all three media are assumed to be

the same, we obtain the following approximate expression for the nonretarded Hamaker constant for two macroscopic phases a and c interacting across a medium b:

$$\mathcal{A}_{abc} = \frac{3}{4} k_B T \left(\frac{\epsilon_a - \epsilon_b}{\epsilon_a + \epsilon_b} \right) \left(\frac{\epsilon_c - \epsilon_b}{\epsilon_c + \epsilon_b} \right) + \frac{3h\nu_e}{8\sqrt{2}} \cdot \frac{(n_a^2 - n_b^2)(n_c^2 - n_b^2)}{\sqrt{(n_a^2 + n_b^2)(n_c^2 + n_b^2)} \left[\sqrt{(n_a^2 + n_b^2)} + \sqrt{(n_c^2 + n_b^2)} \right]} \quad (2)$$

Where:

ν_e is the plasma frequency of free-electron gas;

n_a, n_b, n_c are the refractive index of material a, b, and c.

The interface potential on the non-retarded van der Waals free energy interaction between two semi-infinite layers a and c acting across a medium b, as a function of layer separation D (Scheme S2), is:

$$E_{vdw} = -\frac{\mathcal{A}_{abc}}{12\pi} \cdot \frac{1}{D^2} \quad (3)$$

It is important to bear in mind that the DLP theory is a continuum theory, therefore it might only be safely used when the interacting surfaces are farther apart than the molecular dimensions of the surface structures. The systems we considered in our experiments are on the edge of the DLP's limit. The results obtained (See Figure S2) are indeed of qualitative nature only, because the nanostructures on the inorganic layers of the developed coating are on the same scale as the thickness of the lubricant film covering the top region of the inorganic layers.

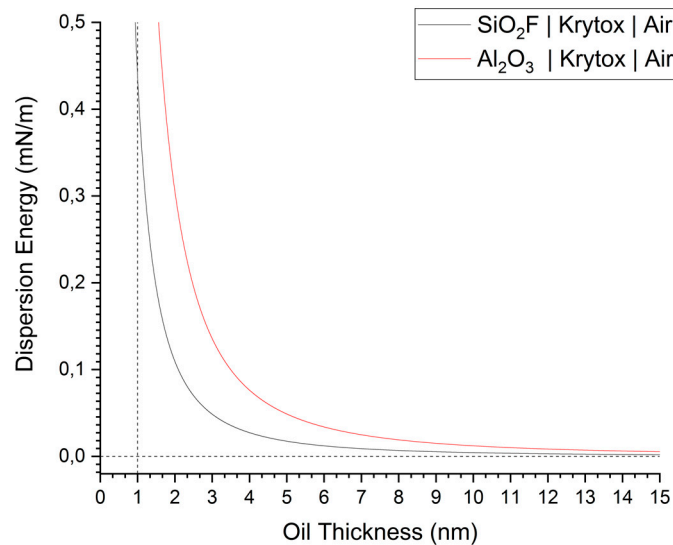


Figure S2. Dispersion energy term vs. Krytox™ lubricant thickness with both Silica and Alumina layers.

References

1. Kajiyama, T.; Schellenberger, F.; Papadopoulos, P.; Vollmer, D.; Butt, H. J. 3D Imaging of Water-Drop Condensation on Hydrophobic and Hydrophilic Lubricant-Impregnated Surfaces. *Sci. Rep.* **2016**, *6*, 1–10.
2. Kralchevsky, P. A.; Nagayama, K. Capillary interactions between particles bound to interfaces, liquid films and biomembranes. *Adv. Colloid Interface Sci.* **2000**, *85*, 145–192.
3. Israelachvili, J. N. *Intermolecular and Surface Forces*, 3rd ed.; Academic Press: Burlington MA, US, **2011**.
4. Owais, A.; Smith-Palmer, T.; Gentle, A.; Neto, C. Influence of long-range forces and capillarity on the function of underwater superoleophobic wrinkled surfaces; *Soft Matter*. **2018**, *14*, 6627–6634.